

# X-ray and Neutron Diffraction Study of Nanocrystalline Ti–Ru–Fe–O Compounds

M. Blouin and D. Guay\*

*INRS-Énergie et Matériaux, 1650 Blvd Lionel-Boulet, C.P. 1020, Varennes, Québec, Canada J3X 1S2*

J. Huot and R. Schulz

*Technologies émergentes de production et de stockage, Institut de recherche d'Hydro-Québec, 1800 Blvd. Lionel-Boulet, C.P. 1000, Varennes, Québec, Canada J3X 1S1*

I. P. Swainson

*Steacie Institute for Molecular Sciences, National Research Council, Chalk River Laboratories, Chalk River, Ontario, Canada K0J 1J0*

*Received April 10, 1998. Revised Manuscript Received July 8, 1998*

The effect of adding oxygen on the structure of nanocrystalline Ti–Ru–Fe compounds obtained by high-energy ball-milling has been studied by X-ray and neutron diffraction using a Rietveld refinement analysis. It is shown that oxygen atoms readily oxidize Ti to form various types of titanium oxides depending on the oxygen content. In each case, a simple cubic structure (*cP2*-CsCl) is also formed during milling but with a concentration higher than expected on the basis of various reaction schemes. Through a detailed analysis of the neutron and X-ray diffraction peaks, it is shown that the 1a site of the CsCl-type unit cell is depleted from Ti atoms by preferential substitution with Fe. At high oxygen concentration, the alloy is a multiphase material containing  $Ti_{2-x}Ru_{1+y}Fe_{1+z}$ , Ti oxides, Ru, and Fe.

## Introduction

The electrolysis of chloride ions, which is the first step in the process of sodium chlorate formation, is plagued with a high overpotential. About 90% of this overpotential originates from the cathodic side of the reaction, where hydrogen evolution occurs, and typically, the cathodic overpotential on mild steel cathodes is on the order of 900 mV. A reduction of this value by 300 mV would cause a 10% reduction in the energy consumption, and therefore, important energy savings could be obtained by developing more efficient cathodes.

Over the years, nanocrystalline materials<sup>1</sup> have demonstrated very interesting behavior, often different from their polycrystalline counterparts. This is believed to be due to the high ratio of surface to bulk atoms, which can vary from 27 to 49% for crystallites of 5 nm, depending on the size of the atoms.<sup>2</sup> These nanocrystalline materials are becoming more and more important in the field of electrochemical-related applications. Thus, nanocrystalline Ni<sup>3</sup> and Ru<sup>4</sup> have shown higher corrosion resistance than their polycrystalline counterparts. Nanocrystalline Ni–Mo-activated cathodes have also shown far superior electrocatalytic activities for the

hydrogen evolution reaction in basic solutions<sup>5</sup> than conventional associated alloys.

There are several ways to prepare nanocrystalline alloys, like the evaporation–condensation technique<sup>2</sup> or the heat-treatment of some amorphous alloys.<sup>6,7</sup> Mechanical alloying is a particularly interesting alternative,<sup>8</sup> since it allows the preparation of metastable alloys with nanosized crystals in quantities large enough to fulfill the requirement of mass production.

It was shown recently that a reduction of the cathodic overpotential for hydrogen evolution under typical chlorate electrolysis conditions of about 250–300 mV could be gained by using ball-milled nanocrystalline Ti<sub>2</sub>RuFe alloy as activated cathode materials.<sup>9</sup> However, during prolonged operation, the Ti<sub>2</sub>RuFe electrodes suffer from decrepitation and fall apart.<sup>10,11</sup> It was found, however, that the mechanical stability could be significantly

(5) Schulz, R.; Huot, J. Y.; Trudeau, M. L.; Dignard-Bailey, L.; Yan, Z. H.; Jin, S.; Lamarre, A.; Ghali, E.; Van Neste, A. *J. Mater. Res.* **1994**, *9*, 2998.

(6) Yamashita, J. *Chem. Soc., Faraday Trans. 1* **1987**, *83*, 2895.

(7) Yoshizawa, J. *Appl. Phys.* **1988**, *64*, 6044.

(8) Fecht, H. J. *Advances in Powder Metallurgy*; MPIF: Princeton, NJ, 1989; Vol. 2, pp 111–122.

(9) Blouin, M.; Guay, D.; Huot, J.; Schulz, R. *J. Mater. Res.* **1997**, *12*, 1492.

(10) Guay, D.; Yip, S.-H.; Irissou, E.; Roué, L.; Blouin, M.; Boily, S.; Huot, J.; Schulz, R. *Nanocrystalline Ti–Ru–Fe–O alloys as cathode materials in the chlorate industry*; International Forum on Electrolysis in the Chemical Industry; Electrolysis Co.: Lancaster, NY, 1996; p 346.

(11) Roué, L.; Irissou, É.; Bercier, A.; Bouaricha, S.; Blouin, M.; Guay, D.; Boily, S.; Huot, J.; Schulz, R. *J. Appl. Electrochem.* Submitted.

\* To whom correspondence should be addressed.

(1) Birringer, R. *Mater. Sci. Eng.* **1989**, *A117*, 33.

(2) Siegel, R. W. *Annu. Rev. Mater. Sci.* **1991**, *21*, 559.

(3) El Kedim, O.; Tachikart, M.; Gaffet, E. *Mater. Sci. Forum.* **1996**, *225–227*, 825.

(4) Roué, L.; Blouin, M.; Guay, D.; Schulz, R. *J. Electrochem. Soc.* **1998**, *145*, 1624.

Table 1. Structural Parameters of the Milled Powders

sample	nominal composition Ti:Ru:Fe:O	phase	lattice parameters		crystallite size (nm)	weight fraction	$R_{wp}/R_e$
			$a$	$c$			
A	2:1:1:0	$Ti_2RuFe$	3.031		7	97	1.32
		Fe	2.873		11	3	
B	2:1:1:1/2	$Ti_2RuFe$	3.024		6	85	1.48
		TiO	4.204		8	6	
		Ru	2.693	4.331	8	3	
		Fe	2.880		8	6	
C	2:1:1:1	$Ti_2RuFe$	3.031		6	72	1.32
		TiO	4.205		5	14	
		Ru	2.736	4.243	11	6	
		Fe	2.881		5	8	

improved by adding oxygen in the alloy without affecting the electrocatalytic activity.<sup>12</sup> Thus, while a  $Ti_2RuFe$  electrode desintegrates after 100 h of electrolysis in chlorate electrolysis conditions, a  $Ti_2RuFeO_2$  electrode withstands more than 300 h of electrolysis without displaying any sign of degradation.<sup>10,11</sup>

From a fundamental point of view, it is important to understand how oxygen could improve the structural integrity. Part of the answer may come from the discovery that  $Ti_2RuFe$  absorbs hydrogen easily and thus forms a hydride.<sup>10,11,13</sup> As shown elsewhere,<sup>11</sup> it is the successive hydriding and dehydriding cycles which are responsible for the poor mechanical stability of the nanocrystalline  $Ti_2RuFe$  alloy. It is thus mandatory to understand how the incorporation of oxygen into the alloy affects these characteristics and, in particular, how the structure and phase composition of the nanocrystalline alloy are affected by the presence of oxygen.

A first effort in that direction was undertaken recently by using X-ray diffraction and Rietveld refinement analysis to unravel the structure and phase composition of ball-milled Ti–Ru–Fe–O.<sup>12</sup> However, XRD presents some inherent limitations that prevent a complete understanding of the structure. In XRD, the scattering power is a function of the atomic number.<sup>14</sup> Thus, while the chemical contrast between Ru and Fe, or Ru and Ti is good, that between Fe and Ti is poor, and oxygen is very difficult to detect. Moreover, most of the phases present in the milled alloy appear in the form of nanometer-sized crystals, thus causing a considerable broadening of the diffraction peaks. This, added to the fact that the stoichiometry of some of these phases may vary over a very wide range, thus causing an additional broadening of the peaks, renders the identification of some oxide phases quite difficult.<sup>12</sup>

In neutron diffraction, the scattering length is not a function of the atomic number.<sup>15</sup> Thus, the chemical contrast between Ti and Ru, or Ti and Fe is good in neutron diffraction. Also, neutron scattering is more sensitive to the presence of oxygen compared to X-ray scattering. In the case of nanocrystalline Ti–Ru–Fe–O alloys, the best approach is certainly to use both X-ray and neutron diffraction analysis in order to get a full picture of the structure and phase composition of the alloy milled in the presence of oxygen.

In this paper, the phase composition and structure of nanocrystalline Ti–Ru–Fe–O compounds will be

determined as a function of the oxygen content for  $x$  ranging from 0.0 to 2.0 by steps of 0.5. This will be done by using X-ray and neutron diffraction analyses and the Rietveld refinement method. It will be shown that oxygen reacts with Ti to form various titanium oxides. This creates a depletion of Ti on the 1a site of the simple cubic structure of  $Ti_2RuFe$  ( $cP2$ -CsCl), which is preferentially filled with Fe. The consequences on the mechanical stability of the alloys used as activated cathode materials in chlorate electrolysis conditions are outlined.

## Experimental Section

Ti, Ru, and Fe (99.5% or higher) from Micron, Alfa-Aesar, and QMP, respectively, were used as starting powders. Oxygen was introduced in the alloys through the addition of  $Fe_2O_3$  (99.0% from Aldrich). TiO (Aldrich 99.9%) was also added to balance the oxygen content. The nominal metallic ratio (Ti:Ru:Fe) was kept constant at 2:1:1. The O content was varied from 0.0 to 2.0 by step of 0.5. Milling was performed in a Spex 8000 mixer/mill using a stainless steel vial (38.1 mm of diameter and 47.6 mm of length), with two 11 mm and one 14 mm diameter balls. The duration of the milling was 40 h. The ball to powder ratio was kept constant at about 4.5:1. Powder handling were performed under a controlled Ar atmosphere in a glovebox to avoid air contamination.

X-ray diffraction diagrams were taken on a Philips XPERT diffractometer using  $Cu K\alpha$  radiation. Neutron diffraction experiments were performed using the C2 DUALSPEC high-resolution neutron powder diffractometer at Chalk River, with a 800-multiwire detector spanning  $80^\circ$  ( $2\theta$ ). The detector floats on an epoxy dance floor using a high-pressure air supply. The monochromator was a planar Si (531) slab, with a reflection at a "take-off" angle of  $92.8^\circ$  (wavelength of 1.3296 Å). The sample holders used were cylindrical and made of vanadium (diameter 0.5 cm, height 7 cm). The Rietveld analysis<sup>16</sup> of neutron and X-ray diffraction data was performed using the GSAS software,<sup>17</sup> which allows the refinement of a single structure model over several diffraction patterns. In the case of the cubic phase, 10 parameters were refined, namely the phase proportion and the lattice constant, two variables to define the peak shape ( $L_x$  and  $L_y$ ) and three parameters (Ti, Ru, and Fe) for each of the two sites occupancies (1a and 1b). In the case of the minor phases (Fe, TiO, and Ru), only three parameters were refined, namely the phase proportion, its lattice constant, and one variable to define the peak shape ( $L_x$ ). The ratio  $R_{wp}/R_e$  with  $R_{wp}$  being the weighted profile difference between the calculated and measured intensities and  $R_e$  being an estimation of the minimum possible value of  $R_{wp}$ , is also given in Table 1. The value of this ratio is an indicator of the "goodness of the fit".

(12) Blouin, M.; Guay, D.; Schulz, R. *Nano. Mater.* In press.

(13) Roué, L.; Guay, D.; Schulz, R. *J. Electroanal. Chem.* Accepted.

(14) Von Dreele, R. B. *Los Alamos Sci.*, **1990**, *19*, 133.

(15) Squires, G. L. *Introduction to the Theory of Thermal Neutron Scattering*; Cambridge University Press: Cambridge, 1978.

(16) Von Dreele, R. B. *The Rietveld Method*; Young, R. A. Ed.; Oxford University Press, Oxford, 1993, p 227–235.

(17) Larson, A. C.; Von Dreele, R. B. GSAS-General Structure Analysis System, Los Alamos National Laboratory Report No. LA-UR 86-748 1986.

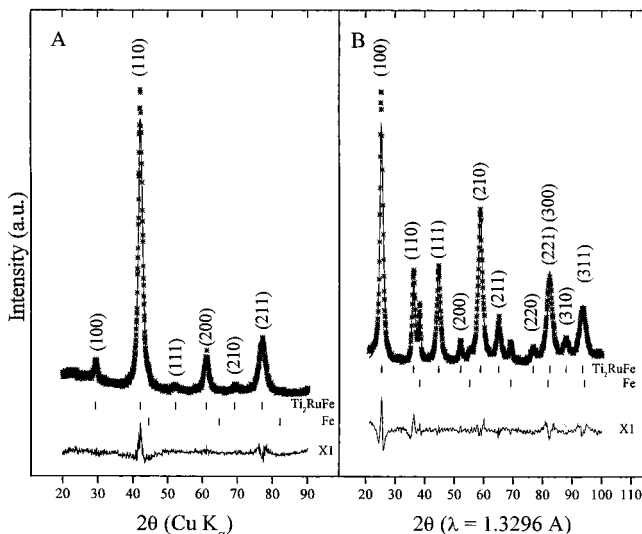


**Figure 1.** X-ray (A) and neutron (B) diffraction patterns of a powder mixture made of Ti:Ru:Fe (2:1:1) milled for 40 h. The peaks are indexed for the  $\text{Ti}_2\text{RuFe}$  ( $cP2\text{-CsCl}$ ) phase.

## Results and Discussion

**Milling of Elemental Powder Mixture.** The X-ray and neutron diffraction patterns of a mixture of elemental Ti:Ru:Fe 2:1:1 are shown in parts A and B of Figure 1, respectively. In these figures, the stars represent the experimental data and the full line is the simulated pattern obtained from the Rietveld refinement analysis. The bars at the bottom indicate the location of the reflection peaks of each phase used in the refinement analysis. The difference (X1) between the measured and the calculated patterns is also shown at the bottom. As will be shown, the main phase found after 40 h of milling has a simple cubic structure ( $cP2\text{-CsCl}$ ). The fundamental (even sum of  $h$ ,  $k$ , and  $l$ ) and the superlattice (odd sum of  $h$ ,  $k$ , and  $l$ ) reflection peaks of that phase are indexed in Figure 1. It is interesting to note that, while the intensity ratio (110)/(100) is higher than unity in the XRD pattern (Figure 1A), this same ratio is smaller than unity in the corresponding neutron diffraction pattern.

The fitting parameters, namely the weight fractions, the lattice parameters, and crystallite sizes of each phase extracted from the simultaneous Rietveld refinement analysis of the X-ray and neutron diffraction patterns, are given in Table 1. The benefits of using both X-ray and neutron diffraction to analyze the phases in the milled powder is evident from a comparison of the diagrams shown in Figure 1. The X-ray diffraction pattern of Figure 1A shows a single series of peaks attributed to  $\text{Ti}_2\text{RuFe}$  ( $cP2\text{-CsCl}$ ). However, on the corresponding neutron diffraction pattern (Figure 1B), reflections from a bcc Fe phase ( $cI2\text{-W}$ ) are also clearly visible, which most probably originates from the erosion of the container and balls occurring during the milling operation. The weight fraction of Fe is 3 wt %, while that of  $\text{Ti}_2\text{RuFe}$  is 97 wt %. The lattice parameter of  $\text{Ti}_2\text{RuFe}$  is 3.031 Å. TiFe and RuTi have a simple cubic structure similar to that of  $\text{Ti}_2\text{RuFe}$ .<sup>18</sup> The lattice parameter of TiFe is (2.97 Å),<sup>19</sup> while that of RuTi is

**Table 2. Site Occupancies of the Simple Cubic Phase**

sample	nominal composition Ti:Ru:Fe:O	site occupancy <sup>a</sup>					
		site 1a (0 0 0)			site 1b ( $1/2$ $1/2$ $1/2$ )		
		Ti	Ru	Fe	Ti	Ru	Fe
A	2:1:1:0	0.89	0.06	0.06	0.07	0.48	0.48
B	2:1:1: $1/2$	0.72	0.07	0.21	0.00	0.61	0.36
C	2:1:1:1	0.76	0.00	0.25	0.00	0.63	0.37
D	2:1:1: $3/2$	0.63	0.00	0.37	0.00	0.61	0.39

<sup>a</sup> The isotropic thermal parameter was assumed to be the same at each site with a value of 0.0112. The sum of the 1a and 1b site occupancies has not been constrained during the refinement process.

(3.06 Å).<sup>20,21</sup> Assuming that the Vegard's law holds true, the stoichiometry of the compound calculated from these lattice parameter values is very close to  $\text{Ti}_2\text{RuFe}$ .

In a perfectly ordered  $cP2\text{-CsCl}$  structure, all the 1a sites are occupied by Ti atoms, while the 1b site are shared by Ru and Fe. This is not the case when  $\text{Ti}_2\text{-RuFe}$  is prepared by ball-milling. The site occupancies of the simple cubic unit cell are given in Table 2. For the oxygen-free sample ( $\text{Ti}_2\text{RuFe}$ ), the occupancy of the 1a site is Ti = 0.889, Ru = 0.061, and Fe = 0.061, while that of the 1b site is Ti = 0.071, Ru = 0.479, and Fe = 0.479. This corresponds to a long-range-order parameter,  $S$ , defined as  $S = (x_{\text{Ti}} - F_{\text{Ti}})/(1 - F_{\text{Ti}})$ , of 0.778, where  $x_{\text{Ti}}$  is the fraction of Ti sites occupied by Ti atoms and  $F_{\text{Ti}} = 0.5$ . Thus, the B2 structure is slightly disordered, which is not uncommon in the case of an alloy obtained by ball-milling.<sup>22</sup>

A time-dependent XRD study of the structural modification and phase formation occurring during the milling of an elemental mixture of Ti:Ru:Fe (2:1:1) was presented elsewhere.<sup>9</sup> After 40 h of milling, it was shown that the powder is mainly composed of  $\text{Ti}_2\text{RuFe}$  (92 wt %), mixed with minor phases of TiO and Ru. The lattice parameter of the cubic phase was 3.030 Å and the 1a site occupancy was Ti = 0.885, Ru = 0.0575, and Fe = 0.0575, while that of the 1b site was Ti = 0.115, Ru = 0.4425, and Fe = 0.4425. These values are very close to those found from the simultaneous Rietveld analysis of both X-ray and neutron diffraction spectra recorded on another sample made under similar conditions. Indeed, the only difference between these two sets of measurements lies in the nature and amount of minor phases mixed with the  $\text{Ti}_2\text{RuFe}$  phase. As shown elsewhere,  $\text{Ti}_2\text{RuFe}$  decomposes to TiO, Ru, and Fe, if the milling is performed in an oxygen containing atmosphere,<sup>12</sup> and thus, small variation in the O content from one batch to the other can explain the difference noted above.

**Effect of the O Content.** The X-ray and neutron diffraction patterns of samples B and C, with composition 2:1:1: $1/2$  and 2:1:1:1, are shown in Figures 2 and 3, respectively. The neutron diffraction patterns of samples D and E, with composition 2:1:1: $3/2$  and 2:1:1:2, are shown in Figure 4, curves A and B, respectively. The X-ray diffraction patterns of samples B and C are not

(18) Murray, J. L. *Alloy Phase Diagram* **1981**, 2, 320.

(19) Pearson's Handbook of Crystallographic data for Intermetallic Phase; Villars, P., Calvert, L. D. Eds.; American Society for Metals: 1985; Vol. 3.

(20) Raub, V. E.; Röscher, E. *Z. Metallkde*, **1963**, 54, 1963.

(21) Jordan, C. B. *J. Metals*, **1955**, 7, 832.

(22) Pochet, P.; Tominez, E.; Chaffron, L.; Martin, G. *Phys. Rev. B*, **1995**, 52, 4006.

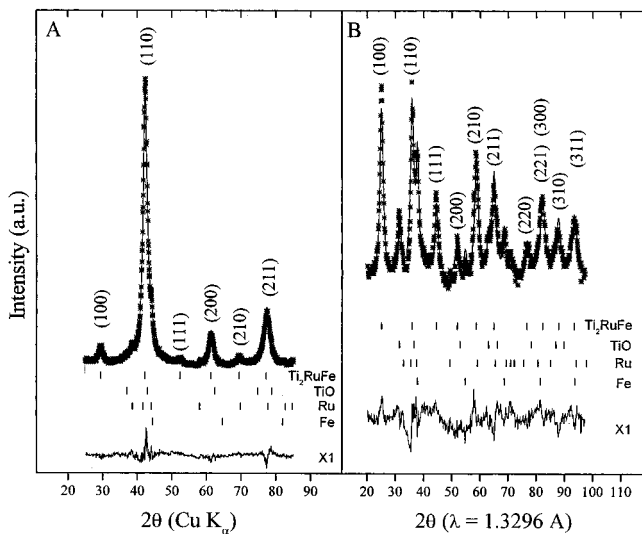


**Figure 2.** X-ray (A) and neutron (B) diffraction patterns of a powder mixture made of Ti:Ru:Fe:O (2:1:1:1/2) milled for 40 h. The peaks are indexed for the  $Ti_2RuFe$  (*cP2-CsCl*) phase.

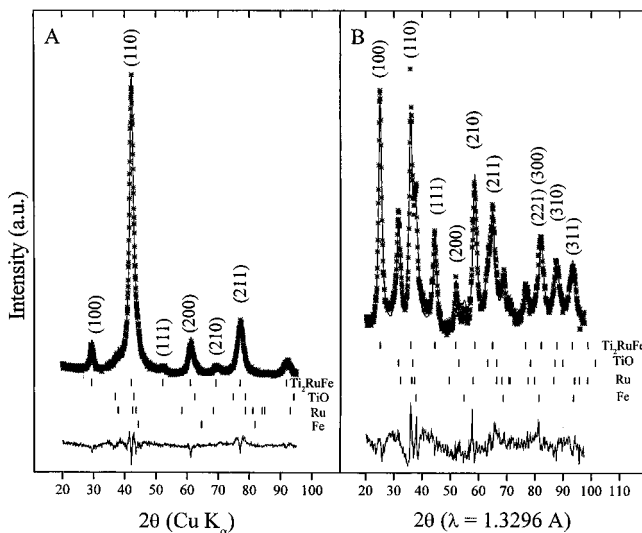


**Figure 3.** X-ray (A) and neutron (B) diffraction patterns of a powder mixture made of Ti:Ru:Fe:O (2:1:1:1) milled for 40 h. The peaks are indexed for the  $Ti_2RuFe$  (*cP2-CsCl*) phase.

significantly different from that of sample A (see Figure 1A), which would suggest that these samples have phase compositions close to each other. However, a completely different picture emerges if the corresponding neutron diffraction patterns are considered. In the case of sample B ( $O = 1/2$ ) (Figure 2B) and sample C ( $O = 1$ ) (Figure 3B), the neutron diffraction patterns unambiguously show that the samples contain a significant fraction of TiO (*cF8-NaCl*) besides the simple cubic phase. The weight fractions of the various phases found in these samples are given in Table 1. It is seen that the weight fractions of TiO, Ru, and Fe increase as the O content of the powder gets larger, with a concomitant decrease in the weight fraction of  $Ti_2RuFe$ .

As mentioned before, it has already been shown that preformed  $Ti_2RuFe$  decomposed to TiO, Ru, and Fe, if it is milled in an oxygen-containing atmosphere,<sup>12</sup> but in that XRD study, no evidence of TiO (and Ru and Fe) could be obtained with less than 5 wt % of O. Titanium oxide phases are, therefore, much more easily detected by neutron than X-ray diffraction.

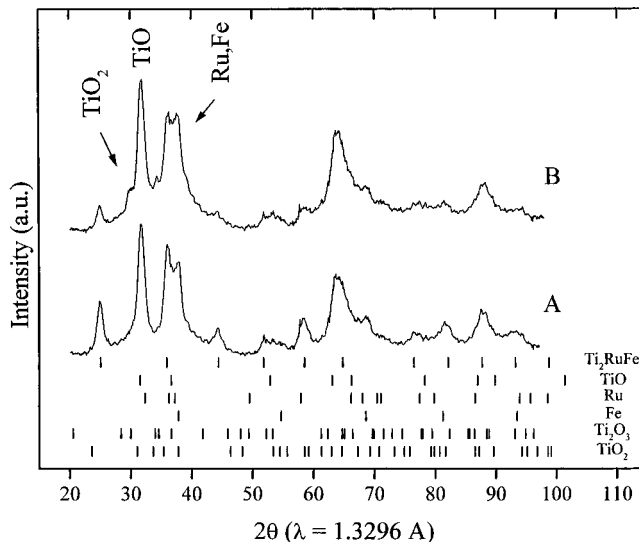


**Figure 4.** Neutron diffraction patterns of a powder mixture with composition made of Ti:Ru:Fe:O 2:1:1:3/2 (A) and 2:1:1:2 (B) milled for 40 h.

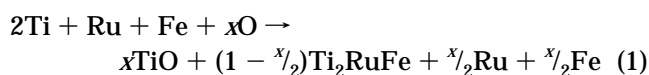
As shown in Table 1, the crystallite size ranges between 5 and 10 nm. The lattice parameter of the B2 phase is similar in samples A and C but slightly lower in sample B.

For sample D ( $O = 3/2$ ) and sample E ( $O = 2$ ), the complete Rietveld refinement analysis has not been performed. However, from Figure 4 the following observations can be made: (i) apparition of diffraction peaks associated with  $Ti_2O_3$  and  $TiO_2$ , (ii) increase in the relative height of the main (111) diffraction peak of TiO, and (iii) relative decrease of the diffraction lines associated with the simple cubic phase. These results indicate that the weight fraction of the simple cubic phase continues to decrease as the oxygen content gets larger, with a concomitant increase of the weight fractions of the various titanium oxide phases.

It is interesting to note that the proportions of Ru and Fe in Table 1 are higher than expected and the proportions of Ti and O are lower than expected. For example, in sample C, the expected proportion of Ru and Fe should be 37.6 and 20.8 wt %, but the calculated proportion based on the Rietveld analysis is 41.8 and 25.3 wt %. On the contrary, Ti and O should be 35.7 and 6.0 wt %, but they are only 29.4 and 3.6 wt %, respectively. This is probably due to undetected Ti oxides like  $Ti_2O_3$  and  $TiO_2$ , which are only visible at higher oxygen concentration (see Figure 4). On the other hand, the Fe/Ru concentration ratio is similar to the expected value.

**Stoichiometry of the B2 Structure.** Up to now, the previous discussion has been conducted by implicitly assuming that the stoichiometry of the simple cubic phase, which was denoted as  $Ti_2RuFe$ , is constant and does not vary with the nominal oxygen content of the powder mixture. This may not be the case.

According to the phase identification made previously, one of the possible reaction sequence occurring during the milling operation is



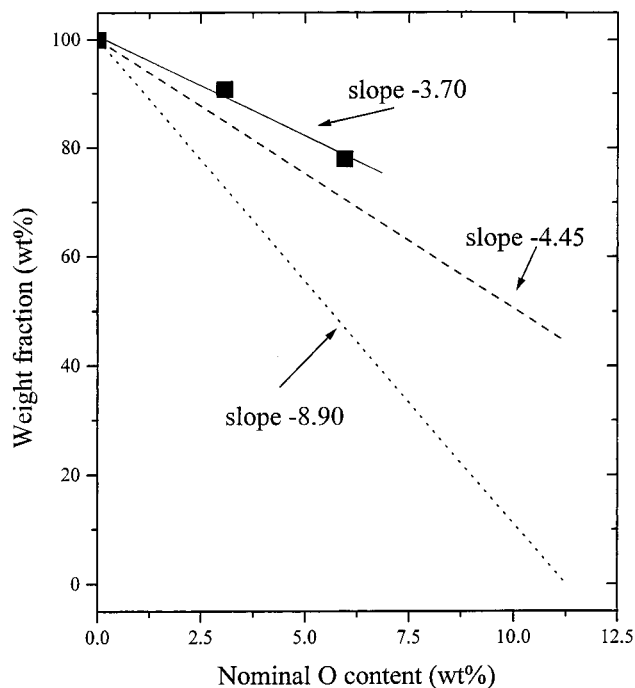
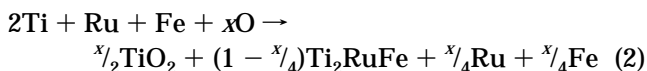


**Figure 5.** Variation of the weight fraction of  $\text{Ti}_2\text{RuFe}$  with the O content. The curves with slopes  $-8.90$  and  $-4.45$  are those expected if  $\text{TiO}$  (reaction 1) and  $\text{TiO}_2$  (reaction 2) oxide phases were formed during the milling process.

According to this reaction, the value of  $\partial([\text{Ti}_2\text{RuFe}])/\partial([\text{O}])$ , the rate at which the weight fraction of  $\text{Ti}_2\text{RuFe}$  decreases with respect to the oxygen content, would be  $-8.9$  (see Figure 5). As shown in Figure 5, the slope of the curve representing the variation of  $[\text{Ti}_2\text{RuFe}]$  with  $[\text{O}]$  is  $-3.7$ , far less steep than expected on the basis of the above reaction. Even in the case where the reaction is assumed to be



which minimizes the amount of Ti atoms reacting with oxygen, the value of  $\partial([\text{Ti}_2\text{RuFe}])/\partial([\text{O}])$  is  $-4.45$ . This is closer to the value found experimentally, but the reaction model is not consistent with the fact that a significant amount of  $\text{TiO}$  is observed in the case of sample B ( $\text{O} = 1/2$ ) and sample C ( $\text{O} = 1$ ). Therefore, these models are not adequate.

It is worthwhile pointing out that the neutron diffraction spectrum of the simple cubic phase shows considerable modification as the oxygen content of the sample is increased. For example, the intensity ratio of the (100) and (110) diffraction peaks decreases from a value larger than unity in the case of sample A (Figure 1B) to a value close to one in the cases of samples B and C (Figures 2B and 3B, respectively) and to a value smaller than one for sample D and sample E (Figure 4). These changes occur in spite of the fact that (i) the lattice parameter of the simple cubic phase does not show any systematic variation (see Table 1) and (ii) the corresponding X-ray diffraction patterns remain pretty much unaffected. We must conclude that some modification in the stoichiometry of the B2 structure and/or in the atomic arrangement must have occurred as a result of the introduction of oxygen in the alloy.

Three are three hypothesis that ought to be considered to explain the previous set of observations:

(1) Oxygen atoms are dissolved into the B2 structure. This is a very appealing hypothesis, since it could also explain the increase structural resistance of  $(2\text{Ti} + \text{Ru} + \text{Fe} + 2\text{O})$  when used as activated cathode for the hydrogen evolution in the chlorate electrolysis.<sup>10,11</sup> As demonstrated elsewhere,  $\text{Ti}_2\text{RuFe}$  readily absorbs hydrogen,<sup>10,11,13</sup> and this induces the decrepitation of electrodes during long-term electrolysis testing.<sup>11</sup> On the contrary, sample D, with  $\text{O} = 2$ , shows a remarkable resistance to decrepitation<sup>11</sup> and it has been suggested that solute O dissolved in  $\text{Ti}_2\text{RuFe}$  might hinder hydrogen absorption and the formation of hydrides.<sup>12</sup>

There are two sites of the B2 structure that can be occupied by oxygen atoms:  $(0 \ 1/2 \ 1/2)$  and  $(0 \ 0 \ 1/2)$ . They correspond to the face and edge centers of the cubic unit cell, respectively. Depending on whether the  $(0 \ 1/2 \ 1/2)$ ,  $(0 \ 0 \ 1/2)$ , or both the  $(0 \ 1/2 \ 1/2)$  and  $(0 \ 0 \ 1/2)$  sites are occupied, the intensity ratio (100)/(111) should increase, decrease, or remain constant as the site occupancy factor goes from 0 to 1.<sup>12</sup> In all cases, the intensity of the (002) peak should increase. In the neutron diffraction patterns, there is no significant variation in the intensity ratio (100)/(111) and no marked increase of the (002) peak. This would suggest that the amount of solute O dissolved in  $\text{Ti}_2\text{RuFe}$  is low. This is consistent with what was previously found from X-ray diffraction analysis alone.<sup>12</sup>

(2) A second hypothesis that needs to be considered is the presence of chemical disorder in the B2 structure induced by oxygen. In the ordered simple cubic structure of stoichiometric  $\text{Ti}_2\text{RuFe}$ , the 1a site of the unit cell is occupied by 1 Ti atom and the 1b site by 0.5 Ru and 0.5 Fe atom. In the case of the fully disordered structure, both the 1a and 1b site occupancies would be 0.5Ti + 0.25 Ru + 0.25 Fe. This would then be identical to a body centered unit cell where the diffraction peaks belonging to the superstructure disappear and the intensity ratio (100)/(110) vanishes. However, the decrease of the (100)/(110) is not observed in the X-ray diffraction pattern of the samples as in the neutron case, and therefore, this hypothesis is not applicable.

(3) The last hypothesis that could be considered is a depletion of Ti atoms from the B2 structure and its replacement by either Fe or Ru. This hypothesis fits most closely with the experimental diffractograms and will serve later on to explain the increased stability of the oxygen-containing nanocrystalline compounds. Substitution of Ti by either Fe or Ru would cause a variation of the superlattice peak intensities, since the form factor of these peaks is proportional to  $([\text{Ti}]f_{\text{Ti}} + [\text{Fe}]f_{\text{Fe}} + [\text{Ru}]f_{\text{Ru}})1a - ([\text{Ti}]f_{\text{Ti}} + [\text{Fe}]f_{\text{Fe}} + [\text{Ru}]f_{\text{Ru}})1b$ , where the  $[\text{Ti}]$ ,  $[\text{Fe}]$ , and  $[\text{Ru}]$  are concentrations of each species on the 1a and 1b sites, and the  $f$  values are the scattering factors of the various elements. In neutron scattering,  $f_{\text{Fe}}$  and  $f_{\text{Ru}}$  are positive and almost identical, while  $f_{\text{Ti}}$  is negative. So, depleting Ti from one site and replacing it by either Fe or Ru will have a marked effect on the intensity of the superlattice peaks of the neutron diffraction pattern. In the case of X-ray diffraction, the scattering factor ( $f$ ) is a function of the atomic number, and thus, replacing Ti ( $Z = 22$ ) by Fe ( $Z = 26$ ) will not

have a marked effect on intensities while it will if Ru replaces Ti in the B2 structure. Since the intensity of the (100) peak (superlattice) is substantially affected in the neutron diffraction patterns but only marginally in the XRD patterns, substitution of Ti by Fe in the B2 structure is favored.

The diffraction patterns of the various samples have been analyzed along these lines, and values of site occupancies for the B2 structure are listed in Table 2. It can be seen that there is effectively a depletion of Ti atoms from the B2 structure. On the 1a site, the Ti occupancy factor decreases from 0.889 to 0.633 as the O content increased from 0 to 1.5, with a concomitant increase of the occupancy factor of Fe from 0.061 to 0.373. In contrast, the Ru occupancy factor on the 1b site increases with the O content. So, in the case of sample D ( $O = 3/2$ ), the composition of the B2 phase, as determined from the simultaneous Rietveld refinement analysis of both X-ray and neutron diffraction patterns, is  $Ti_{1.26}Ru_{1.2}Fe_{1.5}$ . Thus, upon introduction of oxygen in to the powder mixture, various titanium oxides are formed. The weight fraction of the B2 phase in the powder mixture does not decrease as fast as expected because Fe replaces Ti in the B2 structure (see Figure 5).

It may be appropriate at this point to discuss the improved structural stability of Ti:Ru:Fe:O 2:1:1:2 compared to the oxygen-free alloy when used as activated cathode under chlorate electrolysis conditions. It is possible that titanium oxides impart an increase stability to the ensemble by impeding hydrogen absorption during cathodic polarization and by improving corrosion resistance at open circuit potential. It is also possible that the B2 phase whose composition is  $Ti_{2-x}Ru_{1+y}Fe_{1+z}$ , where  $x$ ,  $y$  and  $z$  increase with the oxygen content, absorbs less hydrogen because of the reduced Ti content and, thus, does not be decrepitate during the successive cycles of hydrogen discharge and

open-circuit conditions. This hypothesis is consistent with hydrogen absorption measurements which show that nanocrystalline Ti:Ru:Fe:O 2:1:1:2 does not absorb hydrogen from the gas phase.<sup>10</sup> The experiments to confirm that this observation holds true in the case of hydrogen produced electrolytically are presently underway. This hypothesis certainly makes sense in view of the fact that the stability of the hydride in the  $Ti_{2-x}Ru_{1+y}Fe_{1+z}$  cubic phase should be directly proportional to the Ti content (the enthalpy of formation of FeH, RuH, and TiH being +4, +11, and -38 kJ/mol of atoms, respectively).<sup>23</sup> We are currently trying to synthesize cubic phases with stoichiometry  $Ti_{2-x}Ru_{1+x/2}Fe_{1+x/2}$  without the involvement of O. The first results are encouraging, but a full analysis of the data is yet to come.

### Conclusion

An investigation of the structure of nanocrystalline Ti-Ru-Fe-O alloys with increasing O content was conducted by simultaneous X-ray and neutron diffraction analysis. It was shown that (i) the Ti atoms oxidize to  $TiO$  and then to  $Ti_2O_3$  and  $TiO_2$  as the oxygen content increases. (ii) the weight fraction of the B2 phase does not decrease as fast as expected when the oxygen content increases. This is due mostly to the fact that Fe replaces Ti on the 1a site of the unit cell. At  $O_{1.5}$ , the composition of the B2 phase is  $Ti_{1.26}Ru_{1.2}Fe_{1.5}$ . (iii) the enhanced structural stability of the oxygen-containing nanocrystalline alloy used as cathode material for the synthesis of sodium chlorate may be due to the depletion of Ti in the B2 structure, which reduces hydrogen absorption and material decrepitation during successive hydrogen discharge and open-circuit conditions.

**Acknowledgment.** This work was supported by the Natural Sciences and Engineering Research Council of Canada and Hydro-Québec. M.B. also thanks FCAR-Québec for a student fellowship.

CM980272P

(23) deBoer, F. R.; Boom, R.; Mattens, W. C. M.; Miedema, A. R.; Niessen, A. K. *Cohesion in Metal*; North-Holland Physics Publishing: New York, NY, 1989.